Synthesis and Use in Asymmetric Hydrogenations of Solely Planar Chiral 1,2-Disubstituted and 1,2,3-Trisubstituted Ferrocenyl Diphosphines: A Comparative Study

Yaping Wang and Walter Weissensteiner*

Institute of Organic Chemistry, University of Vienna, Währinger Strasse 38, A-1090 Vienna, Austria

Felix Spindler

Solvias AG, Catalysis Research, P.O. Box, CH-4002 Basel, Switzerland

Vladimir B. Arion§

Institute of Inorganic Chemistry, University of Vienna, Währinger Strasse 42, A-1090 Vienna, Austria

Kurt Mereiter§

Institute of Chemical Technologies and Analytics, Vienna University of Technology, Getreidemarkt 9/164SC, A-1060 Vienna, Austria

Received April 26, 2007

A total of 12 enantiopure 1,2-disubstituted and 1,2,3-trisubstituted ferrocenyl diphosphines [1-Ph_2P-2-R_2PCH_2-3-R′-Fc, R = Cy, *t*-Bu, 3,5-$(CH_3)_2C_6H_3$), R′ = H, CH_3, Ph, 3,5-$(CH_3)_2C_6H_3$)] have been synthesized, characterized, and tested in asymmetric rhodium- and ruthenium-catalyzed hydrogenations of four alkenes and two ketones. The performance of these ferrocene derivatives in catalytic hydrogenations was compared to those of catalysts based on Josiphos, PPF-*t*-Bu_2, and Xyliphos [1-Ph_2P-2-$R_2P(CH_3)$-CH-Fc, R = Cy, *t*-Bu, 3,5-$(CH_3)_2C_6H_3$)]. Dichloro palladium(II) complexes of Xyliphos and its analogues lacking the stereogenic center were synthesized as model compounds, and their molecular structures were studied in solution and, for four complexes, in the solid state. In hydrogenation reactions the replacement of Xyliphos as the catalyst ligand with its analogues lacking the stereogenic center leads to changes in product configurations or significant increases or decreases in ee values.

Introduction

Since the pioneering work of Kumada and Hayashi in 1974,[1] chiral ferrocenyl-based diphosphines have seen enormous development and now constitute a class of catalyst ligands that give outstanding performance in a wide variety of enantioselective reactions.[2,3] Among these systems, Josiphos-type diphoshines are certainly the most prominent examples, mainly since three representatives [Josiphos, **1**; PPF-*t*-Bu_2, **2**; and Xyliphos, **3** (Chart 1)] are used in industrial hydrogenation processes.[4,5] In recent years, these successful applications of Josiphos-type ligands have boosted the further development of ferrocenyl-based diphosphines, and this has led to a number of novel ligands with backbones that are either closely related to that of Josiphos (for example, diphosphine **4**)[6] or have more extended backbones (for example, Taniaphos, **5**,[7] or Walphos-type ligands, **6**).[8] Even small changes in ligand structure have a marked influence on catalytic performance, and as a result, tuning ligands with respect to their electronic and steric properties is a necessary task in catalyst optimization. While electronic properties are usually changed by attaching electron-withdrawing or electron-donating substituents to either the ligand backbone or, more frequently, the phosphine substituents, changes in steric properties can be achieved by a number of different methods. These include changes in the size of phosphine substituents, addition of buttressing substituents in close proximity to the phosphine units, or limiting or enhancing the conformational flexibility of the ligand backbone.[9−12] Recently, in our search for novel ligand backbones, we questioned whether restricting the conformational flexibility of Josiphos-type ligands by transforming the ethyl side chain into either a homo- or heteroannular bridge (e.g., ligands **7** and **8**)

* Corresponding author. E-mail: Walter.Weissensteiner@univie.ac.at.
§ Crystallography.

(1) Hayashi, T.; Yamamoto, K.; Kumada, M. *Tetrahedron Lett.* **1974**, 4405.
(2) Jacobsen, E. N., Pfaltz, A., Yamamoto, H., Eds. *Comprehensive Asymmetric Catalysis, Vol I-III*; Springer: Vienna, 1999.
(3) Ojima, I., Ed. *Catalytic Asymmetric Synthesis*; Wiley-VCH: Weinheim, 2000.
(4) Blaser, H. U., Schmidt, E., Eds. *Asymmetric Catalysis on Industrial Scale: Challenges, Approaches and Solutions*; Wiley-VCH: Weinheim, 2004.
(5) Blaser, H.-U.; Brieden, W.; Pugin, B.; Spindler, F.; Studer, M.; Togni, A. *Top. Catal.* **2002**, *19*, 3.
(6) Yasuike, S.; Kofink, C. C.; Kloetzing, R. J.; Gommermann, N.; Tappe, K.; Gavryushin, A.; Knochel, P. *Tetrahedron: Asymmetry* **2005**, *16*, 3385.
(7) Ireland, T.; Grossheimann, G.; Wieser-Jeunesse, C.; Knochel, P. *Angew. Chem., Int. Ed.* **1999**, *38*, 3212.
(8) Sturm, T.; Weissensteiner, W.; Spindler, F. *Adv. Synth. Catal.* **2003**, *345*, 160.
(9) Gomez Arrayás, R.; Adrio, J.; Carretero, J. C. *Angew. Chem., Int. Ed.* **2006**, *45*, 7674.
(10) Atkinson, R. C. J.; Gibson, V. C.; Long, N. J. *Chem. Soc. Rev.* **2004**, *33*, 313.
(11) Colacot, T. J. *Chem. Rev.* **2003**, *103*, 3101.
(12) Togni, A., Hayashi, T., Eds. *Ferrocenes: Homogeneous Catalysis, Organic Synthesis, Materials Science*; VCH: Weinheim, 1995.

10.1021/om700405a CCC: $37.00
Publication on Web 06/12/2007

Chart 1

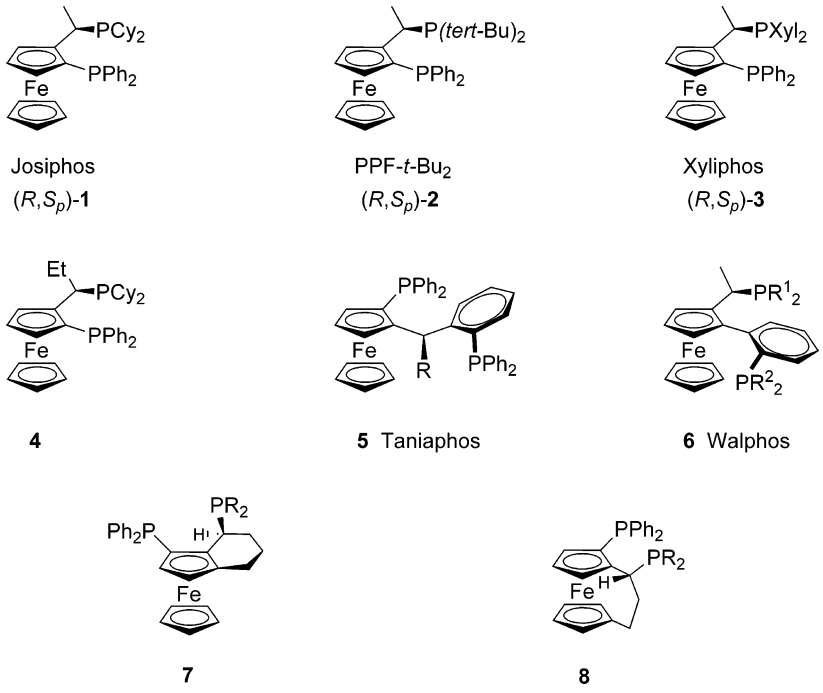

Chart 2

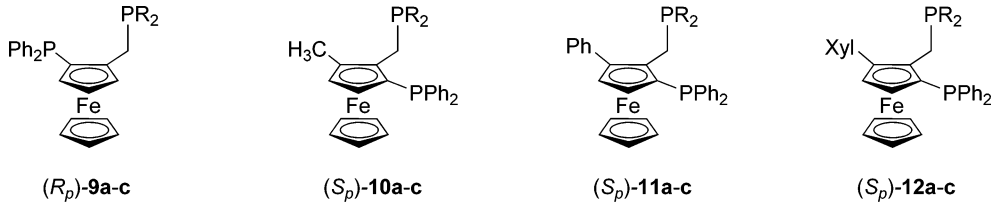

a R = Cy
b R = *tert*-Bu
c R = Xyl = 3,5-$(CH_3)_2C_6H_3$

could influence catalytic performance.[13] The results obtained for a number of hydrogenation reactions supported the view that catalysts expected to perform successfully with different substrates, or even in a range of different reactions, require a controlled flexibility rather than very stiff ligand backbones.

A few years ago, Kagan's group prepared very close analogues of Josiphos-type ligands with planar chirality as the sole source of chirality (e.g., ligands **9a** and **9b**, Chart 2).[14] In hydrogenation reactions, high enantioselectivities were obtained only for a very limited number of alkenes (e.g., for itaconic acid or methyl itaconate), and in general the scope of these diphosphines seems to be much more limited than that of the parent Josiphos-type ligands.

In view of our previous results on homo- or heteroannular bridged ligands **7** and **8**[13] we considered how the lack of a stereogenic center in ligands **9** would actually be reflected in the catalyst performance. For **9** and Josiphos-type ligands one might imagine that in the formation of transition metal complexes the flexibility of the chelate ring or equilibria of chelate ring conformers are strongly influenced by the presence or absence of a stereogenic center and substituents thereon, especially when such a stereogenic center is part of the chelate ring itself. In addition, we wondered whether one could also exert an influence on the chelate ring conformations or on conformer equilibria by attaching additional Cp substituents in close proximity to the chelate ring and how such structural changes would be reflected in the catalyst performance. Therefore, it seemed to be of interest to study the influence of Cp substituents in position 3 on the conformational flexibility and enantioselectivity and to ascertain whether this could provide an additional parameter for ligand tuning.

We report here the synthesis of one 1,2-disubstituted (**9c**) and nine 1,2,3-trisubstituted (**10**−**12**) ferrocenyl diphosphines (Chart 2), all of which are analogues of the 1,2-disubstituted diphosphines **9a** and **9b**. In addition, in order to study the coordination behavior of such ligands, dichloro palladium(II) complexes of Xyliphos (**3**), i.e., **9c**, **10c**, **11c**, and **12c**, were prepared. Structural features of these new ligands and complexes are described along with a number of catalysis results obtained with ligands **9**−**12** in different asymmetric hydrogenation reactions of alkenes and ketones. The data obtained are compared to those of Josiphos-type ligands **1**−**3**.

Results and Discussion

Synthesis of Diphosphines 9−12 and Dichloro Palladium-(II) Complexes of Ligands 3 and 9c−12c. In most cases,

(13) Sturm, T.; Weissensteiner, W.; Spindler, F.; Mereiter, K.; López-Agenjo, A. M.; Manzano, B. R.; Jalón, F. A. *Organometallics* **2002**, *21*, 1766.

(14) Argouarch, G.; Samuel, O.; Kagan, H. B. *Eur. J. Org. Chem.* **2000**, 2885.

Scheme 1

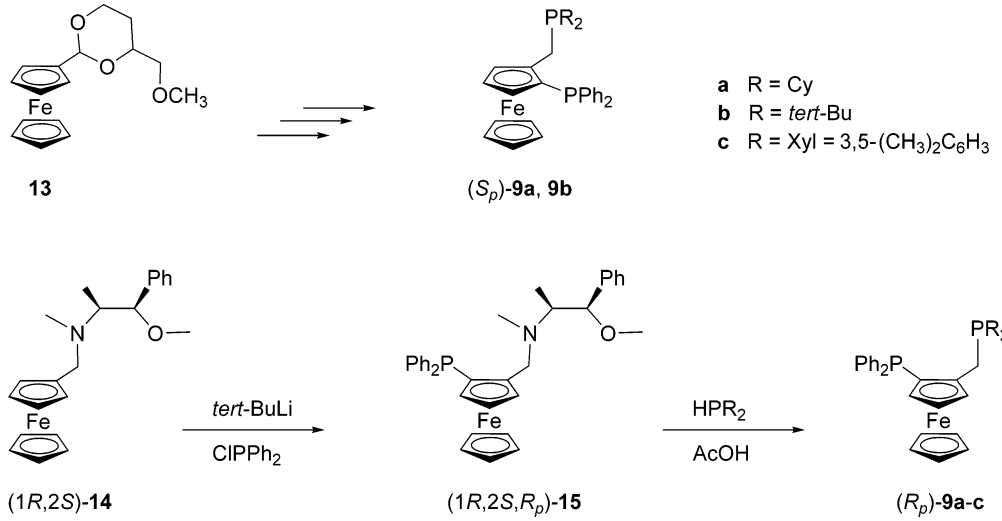

Scheme 2

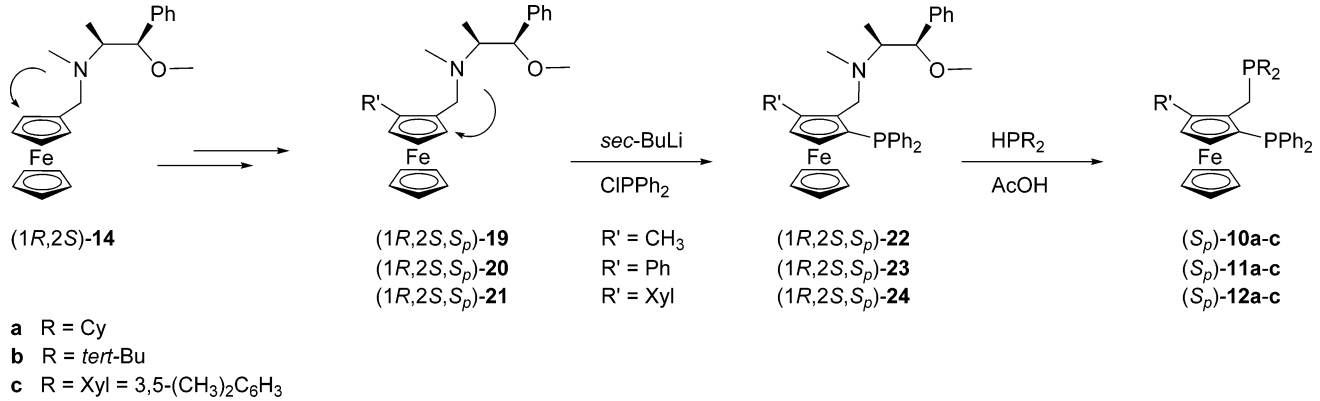

enantiopure 1,2-disubstituted ferrocene derivatives are synthesized enantioselectively from a monosubstituted prochiral precursor or diastereoselectively from a chiral starting material through an *ortho*-directed reaction in which chiral auxiliaries are frequently used as the *ortho*-directing group.[15,16] Originally, diphosphines **9a** and **9b** and related derivatives were synthesized by Kagan and co-workers by applying the latter approach.[14] A chiral acetal, **13**, was used as the starting material (Scheme 1, top). Subsequently, in order to shorten the synthesis, we replaced **13** by *O*-methylephedrine derivative **14**, and this approach has also been used here for the preparation of the novel Xyliphos analogue **9c**.[17]

We started the synthesis of diphosphine **9c** from enantiopure (1*R*,2*S*,R_p)-*N*-[(2-diphenylphosphino)ferrocenylmethyl]-*O*-methylephedrine (**15**), which we previously obtained from (1*R*,2*S*)-*N*-ferrocenylmethyl-*O*-methylephedrine (**14**)[17] and chlorodiphenylphosphine in 81% yield (Scheme 1). In the subsequent step, reaction of **15** with bis(3,5-dimethylphenyl)phosphine in acetic acid resulted in the final diphosphine (R_p)-**9c** (72%).

All of the trisubstituted ligands (**10**−**12**) were prepared according to the same general synthesis route, which is depicted in Scheme 2. In the first reaction sequence, which started from *ortho*-directing *O*-methylephedrine derivative **14**, substituents R′ were introduced in two or three steps to give the 1,2-disubstituted derivatives **19**, **20**, and **21** [R′ = CH_3, Ph, 3,5-$(CH_3)_2C_6H_3$]. In another *ortho*-directed step, a diphenylphosphino unit was attached to the second *ortho*-position next to the chiral auxiliary *O*-methylephedrine. Finally, reaction of each of the trisubstituted ferrocenyl phosphino intermediates **22**, **23**, and **24** with dialkyl and diaryl phosphines R_2PH [R = Cy, *t*-Bu, 3,5-$(CH_3)_2C_6H_3$] in acetic acid led to the replacement of the chiral auxiliary and resulted in the final diphosphines **10a**−**10c**, **11a**−**11c**, and **12a**−**12c** [**10**, **11**, **12**: R′ = CH_3, Ph, 3,5-$(CH_3)_2C_6H_3$; **a**, **b**, **c**: R = Cy, *t*-Bu, 3,5-$(CH_3)_2C_6H_3$].

The 1,2-disubstituted intermediates **19**, **20**, and **21** were synthesized by two different routes. The methyl group was introduced in a three-step sequence (Scheme 3), while the aryl groups were attached using only two steps (Scheme 4). Although derivative **19** (R′ = CH_3) could be prepared easily in one step by reacting **14** in pentane with *t*-BuLi followed by methyl iodide, separation of **19** from unreacted **14** proved to be rather difficult. For this reason, a more convenient three-step sequence was chosen (Scheme 3). In the first step, (1*R*,2*S*)-**14** was lithiated as described above and treatment with dimethylformamide as the electrophile gave aldehyde (1*R*,2*S*,R_p)-**16** in 89% yield. Reduction with $NaBH_4$ in ethanol gave alcohol (1*R*,2*S*,R_p)-**17** (98%), which was further reduced with triethylsilane under acidic conditions[18] to give intermediate (1*R*,2*S*,S_p)-**19** (79%). Both of the aryl-substituted intermediates **20** and **21** were synthesized from **14** in two steps (Scheme 4). As reported

(15) Clayden, J. *Top. Organomet. Chem.* **2003**, *5*, 251.
(16) Clayden, J. In *Chemistry of Organolithium Compounds*; Rappoport, Z., Marek, I., Eds.; Wiley: Chichester, 2004; pp 495−646.
(17) Xiao, L.; Kitzler, R.; Weissensteiner, W. *J. Org. Chem.* **2001**, *66*, 8912.
(18) Olah, G. A.; Narang, S. C.; Gupta, B. G. B.; Malhotra, R. *Synthesis* **1979**, 61.

Scheme 3

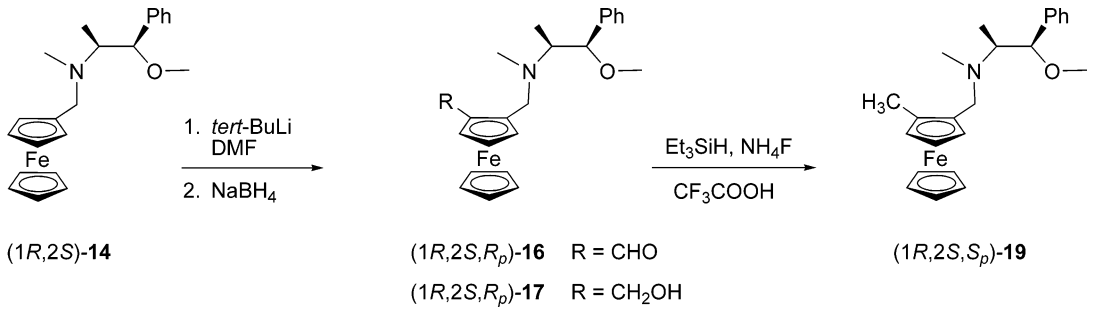

(1*R*,2*S*)-**14** (1*R*,2*S*,R_p)-**16** R = CHO; (1*R*,2*S*,R_p)-**17** R = CH_2OH; (1*R*,2*S*,S_p)-**19**

Scheme 4

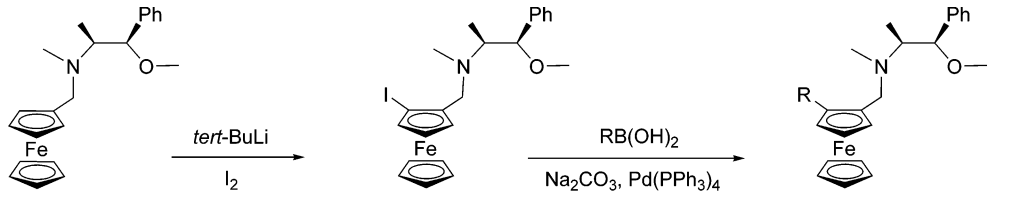

(1*R*,2*S*)-**14** (1*R*,2*S*,R_p)-**18** (1*R*,2*S*,S_p)-**20** R = Ph; (1*R*,2*S*,S_p)-**21** R = Xyl

previously, iodo derivative (1*R*,2*S*,R_p)-**18** is accessible from (1*R*,2*S*)-**14** by *ortho*-lithiation and quenching the reaction mixture with iodine.[17] In the second step, the aryl substituents [R′ = Ph or 3,5-$(CH_3)_2C_6H_3$] were attached to the ferrocene unit in a Suzuki−Miyaura reaction between iodide **18** and either phenyl- or 3,5-dimethylphenylboronic acid.[19] These reactions were carried out in a mixture of toluene and ethanol as the organic solvents, aqueous Na_2CO_3 as the base, and $Pd(PPh_3)_4$ as the catalyst precursor. The use of these conditions gave products (1*R*,2*S*,S_p)-**20** and (1*R*,2*S*,S_p)-**21** in 50 and 80% yield, respectively.

Each of the 1,2-disubstituted derivatives (1*R*,2*S*,S_p)-**19**, (1*R*,2*S*,S_p)-**20**, and (1*R*,2*S*,S_p)-**21** was further reacted in diethyl ether with *s*-BuLi, and the reaction mixture was quenched with chlorodiphenylphosphine to give the 1,2,3-trisubstituted intermediates (1*R*,2*S*,S_p)-**22** (74%), (1*R*,2*S*,S_p)-**23** (69%), and (1*R*,2*S*,S_p)-**24** (84%) (Scheme 2). Finally, reaction of each of these trisubstituted phosphines with dicyclohexylphosphine, di-*tert*-butylphosphine, and bis(3,5-dimethyphenyl)phosphine under acidic conditions resulted in the nine final products **10a**−**10c**, **11a**−**11c**, and **12a**−**12c**, all of which had the S_p absolute configuration.

In order to study the coordination behavior of ligands **3** and **9c**−**12c**, their dichloro palladium(II) complexes [$PdCl_2$(L)], L = (*R*,S_p)-**3**, (R_p)-**9c**, (S_p)-**10c**−(S_p)-**12c**, were prepared by reacting the appropriate diphosphines with dichlorobis(acetonitrile)palladium(II).

The structural integrity of all compounds was assessed by NMR spectroscopy, and in the cases of [$PdCl_2$(L)], L = (*R*,S_p)-**3**, (R_p)-**9c**, (S_p)-**10c**, and (S_p)-**11c**, single crystals were also studied by X-ray diffraction (see below). The ^{31}P NMR spectra of diphosphines **9**−**12** show some interesting features. The signals of the PPh_2 phosphorus directly attached to the Cp ring all lie within a very narrow range of chemical shifts (δ = −22.2 to −23.7 ppm) and are essentially unaffected by the nature of the Cp substituents in position 3. However, the CH_2PR_2 phosphorus signals are rather sensitive to 3-substitution and are shifted to lower field as compared to those of the unsubstituted reference ligands **9** (CH_2PR_2, R = Cy, **12a**: 7.3 versus −1.0 ppm for **9a**; R = *t*-Bu, **12b**: 36.2 versus 27.0 ppm for **9b**; and R = Xyl, **12c**: −7.4 versus −14.3 ppm for **9c**). It is worth noting that—again compared to the unsubstituted diphosphines **9a**−**9c**—a much more marked low-field shift is caused by the methyl group linked to the stereogenic center of Josiphos-type diphosphines **1**−**3** than by the Cp substituents of ligands **10**−**12** [$CH(CH_3)PR_2$, R = Cy, **1**: 15.7 ppm; R = *t*-Bu, **2**: 49.9 ppm; and R = Xyl, **3**: 6.5 ppm].

The assignment of the R_p absolute configuration to **9** and **15**−**18**, as well as the S_p configuration to diphosphines **10**−**12** and intermediates **19**−**24**, is based on the observation that deprotonation of *O*-methylephedrine derivative (1*R*,2*S*)-**14** occurs at the *ortho*-Cp-carbon located counterclockwise to the ephedrine unit (if ferrocene is viewed along an axis defined by the centroid of the substituted Cp ring and the Fe atom; Schemes 1, 3, and 4). This was confirmed previously by chemical correlation[17] and subsequently by X-ray diffraction on complexes [$PdCl_2$(L)], L = (R_p)-**9c**, (S_p)-**10c**, and (S_p)-**11c** (see below). For all monophosphines (**15**, **22**−**24**) and diphosphines (**1**−**3**, **9**−**12**) a negative sign for the specific rotation (measured in $CHCl_3$ at 589 nm) correlates with S_p and a positive sign with the R_p absolute configuration. On complexation of **3**, **9c**, and **10c**−**12c** to the respective dichloro palladium(II) complexes, the specific rotation always changed sign as compared to that of the corresponding free ligand.

Enantioselective Hydrogenations. Diphosphine ligands (R_p)-**9a**−(R_p)-**9c** and (S_p)-**10a**−**c**−(S_p)-**12a**−**c** were tested in catalytic hydrogenations of olefins and ketones (for the catalytic results see Table 1; for substrates tested see Chart 3). For the sake of comparison, all reactions were also run with Josiphos, (*R*,S_p)-**1**, PPF-*t*-Bu_2, (*R*,S_p)-**2**, and Xyliphos (*R*,S_p)-**3**. In performing the hydrogenation reactions we primarily focused on two aspects: (i) on the overall performance and enantioselectivity of the solely planar chiral ligands **9**−**12** as compared to the Josiphos-type ligands **1**−**3** bearing an additional stereogenic center in the side chain and (ii) on the enantioselectivity of complexes of trisubstituted ligands **10**−**12** as compared to the disubstituted ligands **9**. All catalyst precursors were formed *in*

(19) Jensen, J. F.; Søtofte, I.; Sørensen, H. O.; Johannsen, M. *J. Org. Chem.* **2003**, *68*, 1258.

Table 1. Rhodium- and Ruthenium-Catalyzed Hydrogenation of Alkenes and Ketones with Ligands (R,S_p)-3, (R_p)-9, and (S_p)-10−12

substrate			MAC			MCA			DMI			EAC			MPG			EOP		
entry	ligand		conv	ee	conf	conv	ee	conf	conv	ee	conf	conv	ee	conf	conv	ee	conf	conv	ee	conf
1	Josiphos	**1**	100	94	*R*	26	26	*R*	100	99.5	*S*	70	61	*S*	47	23	*S*	17	53	*R*
2	R_{Cp-3} = H	**9a**[a]	100	9	*R*	21	9	*R*	100	98	*S*	64	51	*S*	94	15	*S*	14	26	*R*
3	CH_3	**10a**	100	6	*R*	13	20	*R*	100	99	*S*	20	36	*S*	32	15	*S*	10	50	*R*
4	Ph	**11a**	100	5	*R*	100	21	*R*	100	95	*S*	84	41	*S*	80	12	*S*	1	nd	
5	Xyl	**12a**	100	4	*R*	100	19	*R*	100	97	*S*	85	43	*S*	90	13	*S*	1	nd	
6	PPF-*t*-Bu_2	**2**	25	2	*R*	50	10	*R*	100	10	*R*	48	43	*S*	40	57	*S*	25	29	*R*
7	R_{Cp-3} = H	**9b**[a]	51	16	*R*	57	25	*R*	55	18	*R*	23	31	*S*	39	36	*S*	5	36	*R*
8	CH_3	**10b**	53	6	*S*	46	24	*R*	49	42	*R*	60	44	*S*	38	38	*S*	7	45	*R*
9	Ph	**11b**	51	5	*S*	50	25	*R*	43	25	*R*	20	26	*S*	32	30	*S*	5	25	*R*
10	Xyl	**12b**	22	4	*S*	100	15	*R*	50	37	*R*	40	17	*S*	37	33	*S*	1	nd	
11	Xyliphos	**3**	100	14	*R*	7	8	*R*	96	92	*S*	55	19	*R*	13	3	*S*	10	41	*R*
12	R_{Cp-3} = H	**9c**[a]	100	49	*S*	6	7	*R*	82	21	*S*	42	12	*S*	18	12	*S*	10	nd	
13	CH_3	**10c**	100	67	*S*	4	nd		69	16	*S*	43	27	*S*	15	9	*S*	<5	nd	
14	Ph	**11c**	100	83	*S*	6	nd		54	27	*S*	35	31	*S*	18	6	*S*	17	nd	
15	Xyl	**12c**	100	84	*S*	6	nd		68	24	*S*	34	26	*S*	18	6	*S*	14	26	*S*

[a] For the sake of comparison the absolute configuration of the product is given for ligands with the S_p configuration. For details on reaction conditions and methods of ee determination see the Experimental Section.

Chart 3. Olefins and Ketones Used as Substrates in Catalytic Hydrogenations.

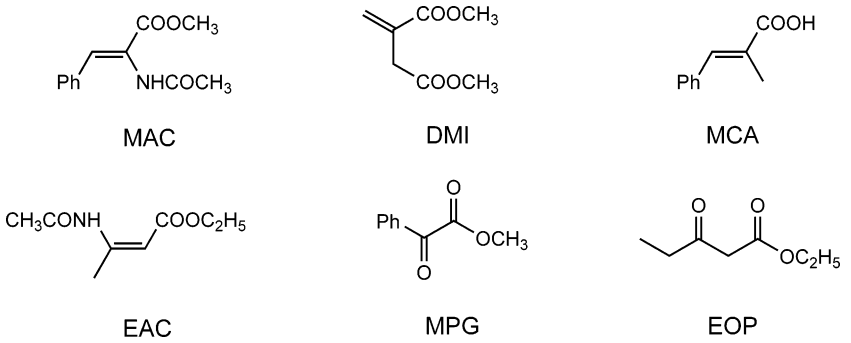

situ using an appropriate Rh or Ru source, and for a given substrate all reactions were carried out under identical reaction conditions (see Experimental Section).

It is well known for the reference ligands **1**−**3** that, under given reaction conditions, only certain catalyst−substrate combinations result in both high conversion and high enantioselectivity. For the substrates tested in our study this is true only for methyl α-(acetamido)cinnamate (MAC) and dimethyl itaconate (DMI) as the substrates and Josiphos (**1**) as the catalyst ligand (Table 1, entry 1) as well as for the combination of DMI and Xyliphos (**3**, Table 1, entry 11). In all other cases either the enantioselectivity or both the conversion and enantioselectivity are low to moderate. In view of these results it was of interest to see how structural changes in **1**−**3**, for example the lack of a stereogenic center (ligands **9a**, **9b**, and **9c**) or the lack of stereogenic center in conjunction with additional Cp substituents (**10**−**12**), would influence the catalytic performance. As one might expect, the influence of structural changes on conversion and enantioselectivity is not uniform. For example, the conversions remained quantitative in the hydrogenation of substrates MAC and DMI on changing from ligand **1** to ligands **9a**−**12a** (Table 1, entries 1−5), whereas with DMI the change from either ligand **2** or **3** to ligands **9b**−**12b** and **9c**−**12c**, respectively, resulted in a slight decrease in conversion (Table 1, entries 6−10 and 11−15). On the other hand, in reactions that were rather slow with reference ligands **1**−**3** the change from **1**, **2**, or **3** to the analogous ligands without a stereogenic center could, in a few cases, give increased conversion. An example of the latter phenomenon is the reaction of MCA with **1** as compared to **11a** and **12a** (Table 1, entries 1, 4, and 5).

As with the conversion, the influence of structural changes in the ligands on enantioselectivity strongly depends on the respective catalyst−substrate combination. In the majority of reactions tested, changing the reference ligands **1**−**3** to their analogues led to only small to moderate changes in enantioselectivity. For example, replacement of catalyst ligand **1** by **9a**−**12a** in the hydrogenation of DMI resulted in neither a significant change in enantioselectivity nor conversion (**1**: 99.5% ee, **11a**: 95% ee; Table 1, entries 1−5). However, in comparison to **1** the reaction of MAC with catalysts modified by the ligands **9a**−**12a** led to a sharp drop in enantioselectivity [from 94% (**1**) to <10% ee; Table 1, entries 1−5], while conversion still remained quantitative. A similar, though less pronounced, drop in enantioselectivity was observed in the hydrogenation of DMI in combination with ligands **3** and analogues **9c**−**12c** [from 92% (**3**) to <28% ee; Table 1, entries 11−15].

Interestingly, the opposite trend was observed in the reaction of MAC with Xyliphos-type ligands. The hydrogenation of MAC with a Xyliphos (**3**)-modified rhodium catalyst gave the corresponding amino acid derivative with only 14% ee, but the use of ligands **9c**−**12c** led to a steady increase in the enantioselectivity to 84% (**9c**: 49%, **10c**: 67%, **11c**: 83%, and **12c**: 84%; Table 1, entries 11−15). In this case the change from Xyliphos to its analogous ligand without a stereogenic center, **9c**, led not only to higher ee values but also to the product with the opposite absolute configuration. The use of (R,S_p)-**3** gave the product of *R* configuration, while use of ligand (S_p)-**9c** resulted in the product of *S* configuration. A similar trend is seen in the hydrogenation of the substrate ethyl (*Z*)-3-(acetamido)crotonate (EAC). The replacement of ligand (R,S_p)-**3** by (S_p)-**9c** again resulted in a change in the product configuration from *R* to *S* (Table 1, entries 11 and 12).

In summary, comparison of the performance of reference ligands **1**, **2**, and **3** with that of their solely planar chiral

analogues **9**−**12** shows that for each of the reference ligands the removal of the stereogenic center is reflected differently. For example, in all hydrogenations tested it was found that catalysts with the reference ligand Josiphos (**1**) gave higher enantioselectivity than those with diphosphines **9a**−**12a**, but, apart from the substrate MAC, changes in ee values remained small (Table 1, entries 1−5). As is the case with Josiphos, replacement of the reference ligand PPF-*t*-Bu_2 (**2**) with its analogues **9b**−**12b** resulted in only small changes in the overall catalyst performance, but in this case, except for the substrate methyl phenylglyoxylate (MPG), slight increases in enantioselectivity were observed (Table 1, entries 6−10). Only when Xyliphos (**3**) was replaced by its analogues **9c**−**12c** were more significant changes found for several substrates. As already mentioned, in the case of DMI this led to a sharp drop in ee values, while for EAC a small decrease and for MAC a very substantial increase in enantioselectivity was found. In addition, in the hydrogenation of substrates MAC, EAC, and ethyl 3-oxo-pentanoate (EOP) the replacement of reference ligand **3** by **9c**−**12c** caused a change in the absolute configuration of the products.

Comparison of ligands **9a**−**c** with their 3-substituted analogues **10a**−**c**−**12a**−**c** shows that the influence of Cp substituents adjacent to the phosphinomethyl unit is rather small. Only in the case of substrate MAC and ligands **9c**−**12c** is a significant increase in ee values observed.

Molecular Structures and Conformational Variability of Complexes [$PdCl_2$(L)] [L = (*R*,S_p)-3, (R_p)-9c, and (S_p)-10c−**12c].** It was observed in the hydrogenation reactions described above that structural changes made to Xyliphos (**3**) as the chiral catalyst ligand, and in particular the removal of its stereogenic center, led to significant changes in ee values. On the basis of this information we questioned how these structural changes in the ligands could be reflected in their respective metal complexes. Therefore, palladium dichloride complexes [$PdCl_2$(L)] of ligands **3** and **9c**−**12c** were prepared as model compounds, and their structures were determined in the solid state (L = **3**, **9c**−**11c**) as well as in solution.

The molecular structures of complexes [$PdCl_2$(L)] [L = (*R*,S_p)-**3**, (R_p)-**9c**, (S_p)-**10c**, and (S_p)-**11c**] were determined in the solid state by X-ray diffraction. Details on X-ray crystallography are given in Table 3 and in the Experimental Section. The absolute configuration of each compound was determined from the X-ray anomalous dispersion effects and was consistent with the chemical evidence. Views of the molecular structures of these compounds are shown in Figures 1 and 2, and selected geometrical data are given in Table 2.

In all solid-state structures of mononuclear metal complexes of Xyliphos (**3**) reported to date Xyliphos acts as a bidentate ligand.[20,21] As in the complex [Ir(cod)((*S*,R_p)-**3**)][BF_4][21] (Figure 1, right), the chelate ring formed on coordination to the metal always adopts a conformation that places the metal unit in an *exo*-position with the phosphorus atom linked to the ferrocenyl ethyl side chain and the metal atom positioned above the substituted Cp ring. In this conformation the carbon atom of the side chain methyl group (C11A) is located almost in the least-squares plane of the substituted cylopentadienyl ring (Cp) and the diphenylphosphino unit is oriented in such a way that one of the phenyl rings (C12−C17) is placed in close proximity to the unsubstituted cylopentadienyl ring (Cp′).

Like Xyliphos (**3**), the analogous diphosphines **9c**, **10c**, and **11c** act as bidentate ligands, but, as compared to [Ir(cod)((*S*,R_p)-**3**)][BF_4], in palladium dichloride complexes [$PdCl_2$(**3**)], [$PdCl_2$(**9c**)], [$PdCl_2$(**10c**)], and [$PdCl_2$(**11c**)] (Figures 1 and 2) the respective chelate rings adopt a totally different conformation, with the palladium dichloride unit now in an *endo*-position. This places both the side chain-linked phosphorus P2 and the palladium atom below the Cp plane. In this conformation one of the xylyl rings (Xyl^2: C24−C29) is positioned in close proximity to Cp′ (for details see Table 2), and this interaction clearly causes significant out-of-plane bending of the methylene carbon C11, to which the dixylylphosphino unit is linked (normal distance of C11 to the Cp least-squares plane: [$PdCl_2$(**3**)] 0.23 Å, [$PdCl_2$(**9c**)] 0.18 Å, [$PdCl_2$(**10c**)] 0.22 Å, [$PdCl_2$(**11c**)] 0.32 Å) as well as an increase in the bond angles C2−C11−P2 to a maximum of 118.1° [$PdCl_2$(**10c**)]. In the case of complex [$PdCl_2$(**3**)], as compared to the *exo* chelate ring conformation of [Ir(cod)((*S*,R_p)-**3**)][BF_4], the *endo* chelate ring conformation is accompanied by a change in the side chain conformation that results in the side chain methyl group being positioned above the substituted Cp ring (normal distance of C11A to the Cp least-squares plane: 1.79 Å). In addition, the Cp rings are slightly tilted against each other, and this tilt also leads to the release of steric strain between Cp′ and the phosphorus-linked Xyl^2 ring. A comparison of the molecular structures of complexes [$PdCl_2$(L)] (L = **9c**, **10c**, and **11c**) shows that attaching substituents to the Cp carbon C3 (ligands **10c** and **11c** as compared to **9c**) leads to an increase in the out-of-plane deformation of C11, which in turn causes the palladium dichloride unit to move closer to the Cp plane (distance between Pd and the Cp least-squares plane: **3** −0.87 Å, **9c** −1.08 Å, **10c** −0.80 Å, **11c** −0.94 Å). This change is associated with a counterclockwise rotation of the diphenylphosphino unit about the P1−C1 bond of about 10° [torsion angle C18−P1−C1−C5: −88.1° (**10c**) and −90.2° (**11c**) versus −99.2° for the enantiomer of **9c**].

In summary, in the solid state the chelate ring in all palladium dichloride complexes [$PdCl_2$(L)] (L = **3**, **9c**, **10c**, and **11c**)

Table 2. Selected Geometrical Parameters of Complexes [$PdCl_2$(L)] (L = (*R*,S_p)-3, (R_p)-9c, (S_p)-10c, and (S_p)-11c)

	3	**9c**	**10c**	**11c**
		Bond Lengths (Å)		
Pd−Cl1	2.351(3)	2.358(1)	2.353(1)	2.363(1)
Pd−Cl2	2.336(3)	2.362(1)	2.343(1)	2.342(1)
Pd−P1	2.214(3)	2.246(1)	2.239(1)	2.251(1)
Pd−P2	2.256(3)	2.256(1)	2.240(1)	2.239(1)
P1−C1	1.813(5)	1.776(2)	1.787(2)	1.793(5)
P2−C11	1.834(9)	1.845(2)	1.846(3)	1.847(5)
C2−C11	1.529(11)	1.490(3)	1.499(3)	1.507(7)
		Bond Angles (deg)		
Cl1−Pd−Cl2	88.6(1)	91.58(2)	91.51(2)	91.64(5)
P1−Pd−P2	93.6(1)	93.50(2)	94.48(2)	94.20(5)
C1−C2−C11	126.1(6)	125.8(2)	125.9(2)	123.5(4)
C3−C2−C11	125.0(6)	125.6(2)	125.1(2)	126.9(4)
C2−C1−P1	128.4(4)	124.5(2)	125.6(2)	125.1(4)
C5−C1−P1	123.4(4)	128.1(2)	126.3(2)	127.0(4)
C2−C11−P2	116.1(6)	117.2(1)	118.1(2)	117.3(3)
C2−C3−C3A			126.4(2)	127.1(4)
C4−C3−C3A			126.3(2)	125.3(4)
		Torsion Angle (deg)		
C18−P1−C1−C5	−88.1(6)	99.2(2)	−88.1(2)	−90.2(5)
		Tilt Angle (deg)		
Cp/Cp′	4.2(2)	5.2(1)	4.7(1)	4.4(2)
		Distance from Least-Squares Plane (Å)		
Pd/Cp	−0.87(2)	−1.081(5)	−0.803(5)	−0.940(11)
P1/Cp	0.11(2)	0.068(3)	0.125(4)	0.056(8)
P2/Cp	−0.53(2)	−0.798(4)	−0.651(5)	−0.631(10)
C11/Cp	0.23(2)	0.183(3)	0.216(4)	0.323(9)
C3A/Cp			0.000(5)	−0.013(9)
H7−Cp′/Xyl^2	2.70(1)	2.553(3)	2.616(3)	2.618(6)

(20) Dorta, R.; Togni, A. *Organometallics* **1998**, *17*, 5441.
(21) Dorta, R.; Broggini, D.; Stoop, R.; Rüegger, H.; Spindler, F.; Togni, A. *Chem.*−*Eur. J.* **2004**, *10*, 267.

Table 3. Details of the Crystal Structure Determinations of Complexes [$PdCl_2$(L)] (L = (R,S_p)-3, (R_p)-9c, (S_p)-10c, and (S_p)-11c)

	[$PdCl_2$(**3**)]·2$C_2H_4Cl_2$[b]	[$PdCl_2$(**9c**)]·1/2$CH_2Cl_2$1/2C_2H_5OH)	[$PdCl_2$(**10c**)]·solv[b]	[$PdCl_2$(**11c**)]·CH_2Cl_2
formula	$C_{44}H_{48}Cl_6FeP_2Pd$	$C_{40.5}H_{42}Cl_3FeO_{0.5}P_2Pd$	$C_{40}H_{40}Cl_2FeP_2Pd$	$C_{46}H_{44}Cl_4FeP_2Pd$
fw	1013.71	867.28	815.81	962.80
cryst size, mm	0.41 × 0.14 × 0.02	0.38 × 0.36 × 0.14	0.37 × 0.18 × 0.16	0.28 × 0.04 × 0.04
space group	$P2_12_12_1$ (no. 19)	$P2_12_12_1$ (no. 19)	$P2_12_12_1$ (no. 19)	$P2_12_12_1$ (no. 19)
a, Å	9.348(3)	11.5451(5)	9.7526(5)	9.7252(5)
b, Å	18.578(6)	17.7582(8)	19.0518(10)	18.5716(10)
c, Å	26.781(9)	18.3153(8)	22.4483(12)	23.1105(14)
V, Å^3	4651(3)	3755.0(3)	4171.0(4)	4174.0(4)
Z	4	4	4	4
ρ_{calc}, g cm^{-3}	1.448	1.534	1.299	1.532
T, K	297(2)	100(2)	100(2)	100(2)
μ, mm^{-1} (Mo Kα)	1.142	1.194	1.008	1.144
F(000)	2064	1768	1664	1960
θ_{max}, deg	25	30	30	28.3
no. of rflns measd	25 035	52 642	61 556	93 507
no. of unique rflns	8142	10 927	12 044	10 379
no. of rflns $I > 2\sigma(I)$	2976	10 802	11 563	8279
no. of params	353	445	420	491
R_1 ($I > 2\sigma(I)$)[a]	0.0778	0.0234	0.0312	0.0497
R_1 (all data)	0.1628	0.0238	0.0331	0.0738
wR_2 (all data)	0.1420	0.0556	0.0756	0.1215
Flack abs str param	−0.06(5)	−0.003(10)	−0.017(12)	−0.02(2)
diff Fourier peaks min./max., e Å^{-3}	−1.01/0.92	−0.40/0.77	−0.71/1.44	−1.19/1.21

[a] $R_1 = \sum||F_o| - |F_c||/\sum|F_o|$, $wR_2 = [\sum(w(F_o^2 - F_c^2)^2)/\sum(w(F_o^2)^2)]^{1/2}$. [b] Disordered solvents (1,2-dichloroethane for [$PdCl_2$(**3**)] and Et_2O/CH_2Cl_2 for [$PdCl_2$(**10c**)]) were squeezed with the program PLATON.[25] Chemical formula and derived quantities for [$PdCl_2$(**10c**)] are given without solvent content.

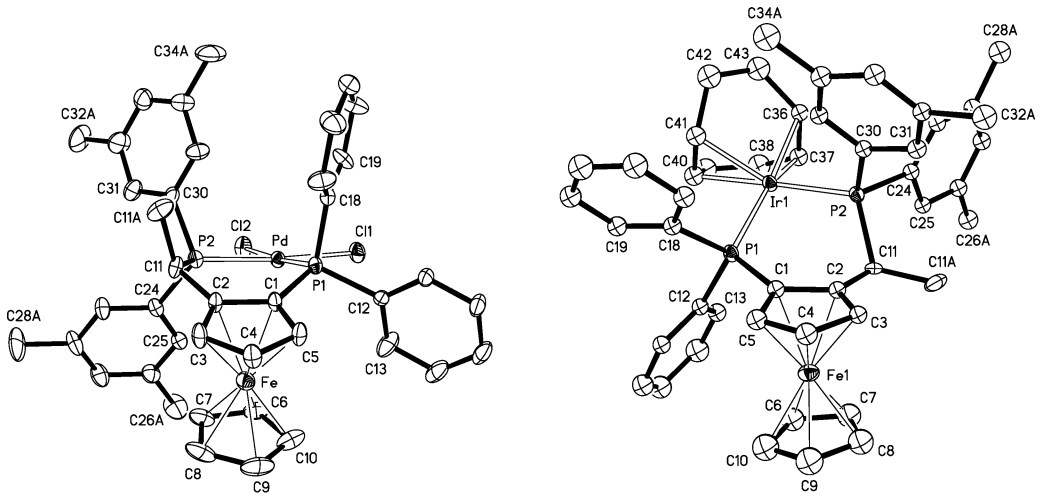

Figure 1. Molecular structures of [$PdCl_2$(**3**)] and [Ir(cod)(**3**)][BF_4] (from ref 21, anion omitted for clarity).

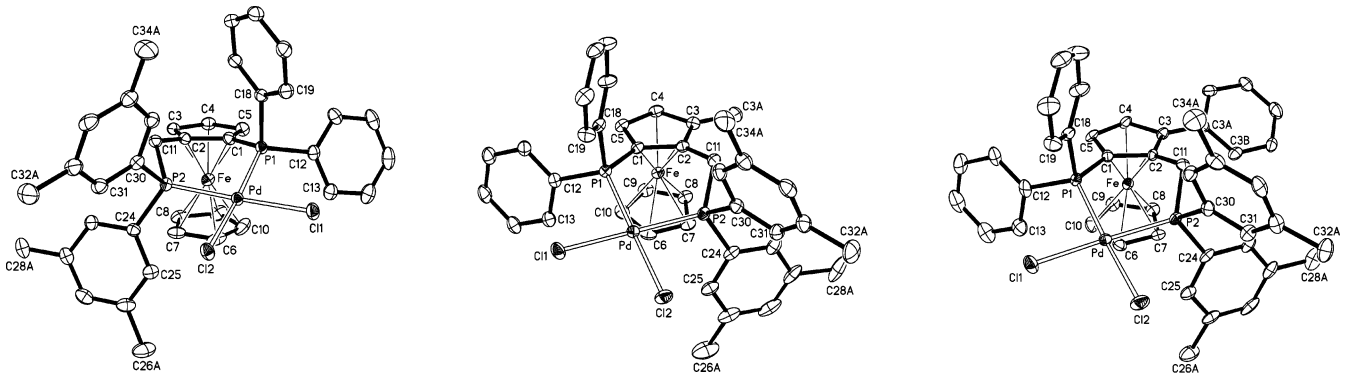

Figure 2. Molecular structures of [$PdCl_2$(L)] (L = **9c**, **10c**, and **11c**) in the solid state.

adopts a conformation in which the palladium dichloride unit is in an *endo*-position. This is particularly striking for the parent ligand Xyliphos (**3**) since in this case the chelate ring conformation depends on the coordinating metal−ligand unit $M(L)_n$. With Ir(cod) ([Ir(cod)(**3**)][BF_4]) the *exo* chelate ring conformation is preferred and with $PdCl_2$ [$PdCl_2$(**3**)] the *endo* conformation

(Figure 1). For complexes of ligands Josiphos (**1**) and PPF-*t*-Bu_2 (**2**) such conformational changes are very unlikely. Regardless of the metal−ligand unit, in the solid state in mononuclear complexes of ligands **1** and **2** the chelate ring has always been found to have an *exo*-conformation. It is clear that the dixylylphosphino unit of **3** is sterically much less demanding than the Cy_2P and *t*-Bu_2P substituents of **1** and **2**, and therefore both *exo* and *endo* chelate ring conformations are feasible. This view is supported by the fact that a chelate ring conformation with the metal unit in an *endo*-position has been reported in one complex of a Xyliphos-related diphosphine ligand, [PdCl(CH_3)(L)] (L = 1-Ph_2P-2-$Ph_2PCH(CH_3)$-Fc), in which the dixylylphosphino group of **3** is replaced by a Ph_2P unit.[22] In complexes of **1** and **2**, in which the chelate ring adopts an *endo*-conformation, one would expect strong steric interactions between one cyclohexyl (**1**) or one *tert*-butyl substituent (**2**) and the respective Cp′ ring, a fact that strongly disfavors the *endo*-conformation.

The replacement of ligand **9c** by either **10c** or **11c** causes comparably small conformational changes—mainly in the chelate ring—and these are attributed to steric interactions between the Cp substituents in position 3 and the dixylylphosphinomethyl side chain. However, the presence of the Cp-C3 substituents CH_3 (**10c**) and Ph (**11c**) seems to have a very similar influence since both complexes [$PdCl_2$(**10c**)] and [$PdCl_2$(**11c**)] have almost identical molecular structures.

The molecular structures of complexes [$PdCl_2$(L)] (L = **3**, **9c**, **10c**−**12c**) in solution were determined by NMR spectroscopy, mainly by analyzing nuclear Overhauser interactions. The assignment of ^1H, ^{13}C, and ^{31}P signals was made using standard one- and two-dimensional techniques. The ^{31}P spectra appear as one would expect; on complexation all phosphorus signals are shifted to lower field by about 40 ppm. However, the main structural information was obtained from proton and predominately from NOESY spectra. On the basis of the results described above one might expect that, as in the solid state, in solution complexes [$PdCl_2$(L)] (L = **3**, **9c**, **10c**−**12c**) could adopt two chelate ring conformations with the palladium dichloride unit either in an *exo*- or in an *endo*-position. Furthermore, dynamic equilibria of such conformers must also be considered. A comparison of the proton NMR spectra of all complexes shows some common features (for the ring and proton numbering see Chart 4). As compared to the free ligands, in each case on complexation the signals of the methyl groups of xylyl ring 1 (Xyl^1) and the Cp-H5 and the Cp′ signals are shifted to higher field, while the methyl protons of xylyl ring 2 (Xyl^2), Cp-H3 (**3** and **9c**), and Cp-H4 (**10c**−**12c**) are shifted to lower field. In addition, for complexes [$PdCl_2$(L)] (L = **9c**, **10c**−**12c**) the CH_2 proton H^{in} (Chart 4) always appears at higher field than the CH_2 proton H^{out}. Significant differences in proton spectra are seen only in the aromatic region. For complexes [$PdCl_2$(L)] (L = **9c**, **10c**−**12c**) the appearance of this region of the spectrum is almost identical, with the signals of the *ortho* protons of xylyl ring 1 (Xyl^1-*ortho*) always located at highest field and the *ortho* protons of xylyl ring 2 (Xyl^2-*ortho*) at lowest field. However, in the case of the Xyliphos complex [$PdCl_2$(**3**)] the appearance of the spectrum is totally different, with the *ortho* protons of phenyl ring 2 (Ph^2-*ortho*) now at lowest field and the Xyl^1-*para* proton at highest field.

Like the ^1H spectra, the NOESY spectra of complexes [$PdCl_2$(L)] (L = **9c**, **10c**−**12c**) also show strong similarities. For complex [$PdCl_2$(**9c**)] the main interactions that cause nuclear Overhauser enhancements are indicated in Chart 4, and most of these interactions are also characteristic of complexes with ligands **10c**−**12c**. In all of these complexes, the observed NOEs are consistent only with a chelate ring conformation with the palladium dichloride unit in an *endo*-position. This follows primarily from the fact that strong interactions between the Cp′ protons and two different rings—one xylyl (Xyl^2) and one phenyl ring (Ph^2)—are observed. For a conformer with the palladium dichloride unit in an *exo*-position, a strong interaction between Cp′ and xylyl *ortho* protons would not be expected since such an arrangement must lead to both xylyl rings being located above the substituted Cp ring.

Chart 4. Numbering Scheme and Main NOE Interactions for [$PdCl_2$(9c)]

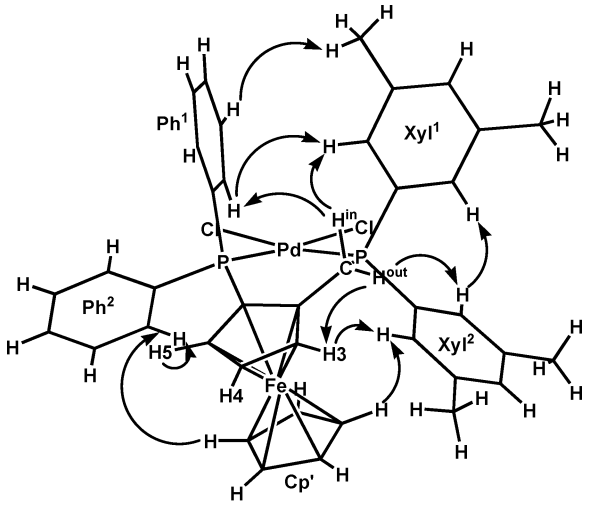

[$PdCl_2$(**9c**)]

However, for the Xyliphos complex [$PdCl_2$(**3**)] the interpretation of the observed set of NOEs is less obvious. In this case the signal of the Cp′ protons overlaps with the signal of the side chain CH proton, and therefore interactions between xylyl *ortho* protons and Cp′ protons (indicative of an *endo* chelate ring conformation) could not be assigned unequivocally. Only one cross-peak between protons of the side chain methyl group and the *otho* protons of one phenyl group allows the differentiation between *exo* and *endo* chelate ring conformations. Such an interaction is expected only when the side chain methyl group [$C(11A)H_3$] is located above the least-squares plane of the substituted Cp ring (as in [$PdCl_2$(**3**)]) and not when this methyl group is located in close proximity to this plane (as in [Ir(cod)(**3**)][BF_4], Figure 1). Therefore, we tentatively assign the *endo*-conformation to the chelate ring of complex [$PdCl_2$(**3**)] in solution.

In summary, in the solid state and in solution all palladium dichloride complexes [$PdCl_2$(L), L = **3**, **9c**−**12c**] adopt a molecular structure in which the chelate ring is in an *endo*-arrangement. In the solid state, both the removal of the side chain methyl group (**9c** versus **3**) and addition of substituents in position 3 of the Cp ring (**10c**, **11c** versus **9c**) lead only to small structural changes. However, the fact that in Xyliphos complexes—depending on the coordinated metal−ligand unit (ML_n)—the chelate ring can adopt both the *exo*- and the *endo*-arrangement seems to indicate a generally higher conformational flexibility for Xyliphos-type complexes as compared to Josiphos- or PPF-*t*-Bu_2-type complexes.

(22) Gambs, C.; Consiglio, G.; Togni, A. *Helv. Chim. Acta* **2001**, *84*, 3105.

Summary

A number of solely planar chiral analogues of ferrocenyl diphosphines Josiphos, **1**, PPF-*t*-Bu_2, **2**, and Xyliphos, **3**, have been tested as catalyst ligands in hydrogenation reactions of four alkenes and two ketones. For these hydrogenations, as compared to catalysts based on the reference ligands **1** and **2**, the influence of ligands lacking the stereogenic center on enantioselectivity was found to be rather small. Only in one case was a severe drop in ee values observed. More significant changes were seen for analogues of Xyliphos. In three cases, the absolute configuration of the product changed when Xyliphos was replaced by ligands without a stereogenic center, and in one case the enantioselectivity dropped significantly. A model study of the molecular structures of dichloro palladium(II) complexes of Xyliphos and analogues revealed that for Xyliphos complexes the conformation of the chelate ring that is formed on complexation of the diphosphine ligand to the metal depends strongly on the co-coordinated metal−ligand unit ML_n. In complexes based on Xyliphos the respective chelate ring can adopt both the *exo*- and the *endo*-conformation. Attempts to use additional Cp substituents for ligand fine-tuning proved successful only in one case. In the hydrogenation of methyl α-acetamido-cinnamate the ee value of 49% obtained with the 1,2-disubstituted ligand **9c** could be increased to 84% on using the 1,2,3-trisubstituted ligand **12c**.

Experimental Section

General Comments. All reactions required inert conditions and were carried out under an argon atmosphere using standard Schlenk techniques. All solvents were dried by standard procedures and distilled before use. ^{1}H, ^{13}C{^{1}H}, and ^{31}P{^{1}H} NMR spectra were recorded on a Bruker DPX-400 spectrometer in $CDCl_3$. Chemical shifts are given relative to $CHCl_3$ (^{1}H: 7.26 ppm), $CDCl_3$ (^{13}C: 77.0 ppm), and 85% H_3PO_4 (^{31}P: 0 ppm). The coupling constants in ^{13}C spectra were due to ^{13}C−^{31}P or ^{13}C−^{19}F coupling. In the ^{1}H NMR data br s, d, t, and q refer to broad singlet, doublet, triplet, and quartet, respectively, and C_q in ^{13}C NMR data stands for quaternary carbon atom. For the signal assignment for complexes [$PdCl_2$(L)] (L = **3c**, **9c**, **10c**, **11c**, or **12c**) the numbering scheme depicted in Chart 4 was used. For all other diphenylphosphino- and dixylylphosphino-substituted derivatives the terms Ph^1, Ph^2 and Xyl^1, Xyl^2 are arbitrarily used to denote the phosphorus-linked phenyl and xylyl rings, respectively. Melting points were determined on a Kofler melting point apparatus and are uncorrected. Mass spectra were recorded on a Finnigan MAT 8230 spectrometer (EI). Optical rotations were measured on a Perkin-Elmer 241 polarimeter. Chromatographic separations were performed under gravity either on silica gel (Merck, 40−62 μm) or on alumina (Merck, activity II−III, 0.063−0.200 mm). Petroleum ether with a boiling range of 55−65 °C was used for chromatography.

Compounds (R_p)-**9a**, (R_p)-**9b**, (1*R*,2*S*)-**14**, (1*R*,2*S*,R_p)-**15**, and (1*R*,2*S*,R_p)-**18** were prepared according to ref 17. For the synthesis of ligands (R_p)-**9c**, (S_p)-**10a**−**c**, (S_p)-**11a**−**c**, and (S_p)-**12a**−**c** and their precursors (1*R*,2*S*,R_p)-**16**, (1*R*,2*S*,R_p)-**17**, and (1*R*,2*S*,S_p)-**19**−**24** see the Supporting Information.

General Procedure for the Synthesis of $PdCl_2$ Complexes. [$PdCl_2$(L)] L = 3c, 9c, 10c, 11c, or 12c. A degassed solution of **3c**, **9c**, **10c**, **11c**, or **12c** (0.1 mmol) in dry benzene (2 mL) was added to a suspension of dichlorobis(acetonitrile)palladium(II) (26 mg, 0.1 mmol) in dry benzene (2 mL) through a Teflon tube. The mixture was stirred for 18 h at rt, and the resulting precipitate was filtered off and washed with benzene (2 × 2 mL) and diethyl ether (3 × 2 mL) to give the palladium complexes as red solids.

[$PdCl_2$((R,S_p)-3)]. Yield: 86%. Mp: dec >270 °C. $[\alpha]_\lambda^{20}$ (nm): +170 (589), +206 (578), +418 (546) (*c* 0.099, $CHCl_3$). ^{1}H NMR (400 MHz): δ 1.00 (dd, 3H, *J* = 14.1 Hz, *J* = 7.3 Hz, CH_3), 2.19 (s, 6H, Xyl^1-CH_3), 2.42 (s, 6H, Xyl^2-CH_3), 3.62 (s, 5H, Cp′), 3.64−3.72 (m, 1H, CH), 3.99−4.03 (m, 1H, Cp−H5), 4.33−4.39 (m, 1H, Cp-H4), 4.40−4.44 (m, 1H, Cp-H3), 6.98 (s, 1H, Xyl^1-*para*), 7.17 (s, 1H, Xyl^2-*para*), 7.27 (d, 2H, *J* = 10.9 Hz, Xyl^1-*ortho*), 7.27−7.32 (m, 2H, Ph^1-*meta*), 7.37−7.44 (m, 1H, Ph^1-*para*), 7.48−7.56 (m, 3H, Ph^2-*meta*, Ph^2-*para*), 7.56−7.63 (m, 2H, Ph^1-*ortho*), 7.71 (d, *J* = 11.9 Hz, Xyl^2-*ortho*), 8.00−8.11 (m, 2H, Ph^2-*ortho*). ^{13}C{^{1}H} NMR (100 MHz): δ 19.90 (d, *J* = 1.5 Hz, CH_3), 21.33 (2C, Xyl^1-CH_3), 21.53 (2C, Xyl^2-CH_3), 32.67 (dd, *J* = 27.0 Hz, *J* = 7.7 Hz, CH), 67.76 (dd, *J* = 57.6 Hz, *J* = 11.5 Hz, Cp-Cq), 69.28 (dd, *J* = 6.9 Hz, *J* = 2.3 Hz, Cp-C4), 70.69 (5C, Cp′), 70.90 (dd, *J* = 7.5 Hz, *J* = 5.0 Hz, Cp-C3), 73.91 (d, *J* = 3.0 Hz, Cp-C5), 92.82 (dd, *J* = 17.6 Hz, *J* = 3.8 Hz, Cp-Cq), 127.40 (d, *J* = 51.6 Hz, Ph-*ipso*), 127.77 (d, 2C, *J* = 11.5 Hz, Ph^2-*meta*), 128.04 (d, 2C, *J* = 11.5 Hz, Ph^1-*meta*), 128.54 (d, *J* = 53.0 Hz, Ph-*ipso*), 130.73 (d, *J* = 3.0 Hz, Ph^1-*para*), 131.24 (d, *J* = 3.0 Hz, Ph^2-*para*), 131.69 (d, *J* = 56.9 Hz, Xyl-*ipso*), 132.11 (d, 2C, *J* = 10.9 Hz, Xyl^1-*ortho*), 132.24 (d, 2C, *J* = 10.9 Hz, Xyl^2-*ortho*), 132.85 (d, *J* = 3.0 Hz, Xyl^1-*para*), 133.42 (d, *J* = 3.0 Hz, Xyl^2-*para*), 134.02 (d, 2C, *J* = 10.7 Hz, Ph^1-*ortho*), 135.30 (d, 2C, *J* = 11.5 Hz, Ph^2-*ortho*), 137.65 (d, 2C, *J* = 11.7 Hz, Xyl-Cq), 138.15 (d, 2C, *J* = 11.7 Hz, Xyl-Cq). Ph-*ipso* and Xyl-*ipso* interchangeable. ^{31}P{^{1}H} NMR (162 MHz): δ +17.11 (d, *J* = 7.9 Hz), +48.59 (d, *J* = 7.9 Hz). Anal. Calcd for $C_{40}H_{40}Cl_2FeP_2Pd$: C 58.89, H 4.94, P 7.59. Found: C 58.67, H 4.85, P 7.50.

[$PdCl_2$((R_p)-9c)]. Yield: 63%. Mp: dec >210 °C. $[\alpha]_\lambda^{20}$ (nm): −265 (589), −311 (578), −608 (546) (*c* 0.074, $CHCl_3$). ^{1}H NMR (400 MHz): δ 2.06 (s, 6H, Xyl^1-CH_3), 2.47 (s, 6H, Xyl^2-CH_3), 2.96 (dd, 1H, *J* = 16.1 Hz, *J* = 7.1 Hz, CH_2-*in*), 3.50 (ddd, 1H, *J* = 16.1 Hz, *J* = 16.1 Hz, *J* = 5.4 Hz, CH_2-*out*), 3.68−3.72 (m, 1H, Cp-H5), 3.71 (s, 5H, Cp′), 4.36 (dd, 1H, *J* = 5.0 Hz, *J* = 2.5 Hz, Cp-H4), 4.37−4.40 (m, 1H, CP-H3), 6.61 (d, 2H, *J* = 12.4 Hz, Xyl^1-*ortho*), 6.88 (s, 1H, Xyl^1-*para*), 7.25 (s, 1H, Xyl^2-*para*), 7.40−7.50 (m, 4H, Ph^1-*meta* + Ph^2-*meta*), 7.50−7.56 (m, 2H, Ph^1-*para* + Ph^2-*para*), 7.69−7.76 (m, 2H, Ph^1-*ortho*), 7.76−7.83 (m, 2H, Ph^2-*ortho*), 8.01 (d, 2H, *J* = 12.4 Hz, Xyl^2-*ortho*). ^{13}C{^{1}H} NMR (100 MHz): δ 21.21 (2C, Xyl^1-CH_3), 21.46 (2C, Xyl^2-CH_3), 28.23 (dd, *J* = 30.7 Hz, *J* = 8.3 Hz, CH_2), 65.60 (dd, *J* = 63.6 Hz, *J* = 10.1 Hz, Cp-Cq), 69.35 (dd, *J* = 6.9 Hz, *J* = 3.5 Hz, Cp-C4), 70.50 (5C, Cp′), 73.14−73.46 (m, 2C, Cp-C3, Cp-C5), 86.40 (d, *J* = 17.6 Hz, Cp-Cq), 127.10 (d, *J* = 54.9 Hz, Ph-*ipso*), 127.57 (d, 2C, *J* = 12.2 Hz, Ph^2-*meta*), 128.95 (d, 2C, *J* = 11.5 Hz, Ph^1-*meta*), 129.32 (d, *J* = 68.1 Hz, Xyl-*ipso*), 129.41 (d, 2C, *J* = 9.9 Hz, Xyl^1-*ortho*), 130.77 (d, *J* = 53.3 Hz, Ph-*ipso*), 131.16, 131.19, 131.23 (2C, Ph-*para*), 132.10 (d, *J* = 57.5 Hz, Xyl-*ipso*), 132.16 (d, *J* = 3.1 Hz, Xyl^1-*para*), 133.67 (d, 2C, *J* = 10.7 Hz, Ph^1-*ortho*), 133.89 (d, 2C, *J* = 11.5 Hz, Xyl^2-*ortho*), 134.04 (d, *J* = 2.3 Hz, Xyl^2-*para*), 134.67 (d, 2C, *J* = 11.5 Hz, Ph^2-*ortho*), 137.79 (d, 2C, *J* = 11.5 Hz, Xyl-Cq), 138.63 (d, 2C, *J* = 12.2 Hz, Xyl-Cq). Ph^1-*meta* and Ph^2-*meta* as well as Ph-*ipso* and Xyl-*ipso* interchangeable. ^{31}P{^{1}H} NMR (162 MHz): δ +20.29 (d, *J* = 7.9 Hz), +28.29 (d, *J* = 7.9 Hz). Anal. Calcd for $C_{39}H_{38}FeP_2$·$PdCl_2$: C 58.42, H 4.78, P 7.73. Found: C 58.18, H 4.88, P 7.59.

[$PdCl_2$((R_p)-10c)]. Yield: 56%. Mp: dec >175 °C. $[\alpha]_\lambda^{20}$ (nm): +50 (589), +50 (578), +150 (546) (*c* 0.006, $CHCl_3$). ^{1}H NMR (400 MHz): δ 1.93 (s, 3H, Cp-CH_3), 2.07 (s, 6H, Ph^1-CH_3), 2.47 (s, 6H, Ph^2-CH_3), 2.77 (dd, 1H, *J* = 15.8 Hz, *J* = 7.4 Hz, CH_2-*in*), 3.54 (ddd, 1H, *J* = 15.8 Hz, *J* = 15.8 Hz, *J* = 5.6 Hz, CH_2-*out*), 3.60 (s, 5H, Cp′), 3.62 (t, 1H, *J* = 2.0 Hz, Cp-H5), 4.33 (t, 1H, *J* = 2.7 Hz, Cp-H4), 6.64 (d, 2H, *J* = 12.4 Hz, Xyl^1-*ortho*), 6.90 (s, 1H, Xyl^1-*para*), 7.26 (s, 1H, Xyl^2-*para*), 7.40−7.48 (m, 4H, Ph^1-*meta* + Ph^2-*meta*), 7.48−7.55 (m, 2H, Ph^1-*para* + Ph^2-*para*), 7.69−7.76 (m, 2H, Ph^1-*ortho*), 7.76−7.82 (m, 2H, Ph^2-*ortho*), 8.04 (d, 2H, *J* = 12.4 Hz, Xyl-*ortho*). ^{13}C{^{1}H} NMR (100 MHz): δ 13.06 (CH_3), 21.23 (2C, Xyl^1-CH_3), 21.47 (2C, Xyl^2-CH_3), 25.91 (dd, *J* = 31.5 Hz, *J* = 8.8 Hz, CH_2), 71.20 (Cp′),

71.41−71.69 (m, 2C, Cp-C4, Cp-C5), 85.35 (d, J = 16.8 Hz, Cp-Cq), 127.00 (d, J = 54.3 Hz, Ph-*ipso*), 127.52 (d, 2C, J = 11.5 Hz, Ph^1-*meta*), 128.91 (d, 2C, J = 11.5 Hz, Ph^2-*meta*), 129.34 (d, J = 68.0 Hz, P-Xyl-*ipso*), 129.48 (d, 2C, J = 9.9 Hz, Xyl^1-*ortho*), 130.23 (d, J = 71.6 Hz, P-Xyl-*ipso*), 131.11 (d, J = 3.0 Hz, Ph^1-*para*), 131.18 (d, J = 3.0 Hz, Ph^2-*para*), 132.07 (d, J = 57.4 Hz, Ph-*ipso*), 132.26 (d, J = 3.0 Hz, Xyl^1-*para*), 133.69 (d, 4C, J = 11.5 Hz, Xyl^2-*ortho*, Ph^1-*ortho*), 133.98 (d, J = 3.0 Hz, Xyl^2-*para*), 134.82 (d, 2C, J = 11.5 Hz, Ph^2-*ortho*), 137.88 (d, 2C, J = 12.3 Hz, Xyl-Cq), 138.74 (d, 2C, J = 11.5 Hz, Xyl-Cq). Ph^1-*meta* and Ph^2-*meta*, Ph^1-*para* and Ph^2-*para*, as well as Ph-*ipso* and Xyl-*ipso*, interchangeable; two Cp-Cq not observed. $^{31}P\{^1H\}$ NMR (162 MHz): δ +22.3 (d, J = 7.9 Hz), +28.7 (d, J = 7.9 Hz).

[$PdCl_2$((*R*$_p$)-11c)]. Yield: 42%. Mp: dec >185 °C. $[\alpha]_\lambda^{20}$ (nm): +209 (589), +257 (578), +504 (546) (*c* 0.067, $CHCl_3$). ^1H NMR (400 MHz): δ 2.09 (s, 6H, Xyl^1-CH_3), 2.57 (s, 6H, Xyl^2-CH_3), 2.62 (dd, 1H, J = 16.1 Hz, J = 6.6 Hz, CH_2), 3.64 (s, 5H, Cp′), 3.68−3.81 (m, 1H, CH_2), 3.81−3.88 (m, 1H, Cp-H5), 4.64 (t, 1H, J = 2.5 Hz, Cp-H4), 6.49 (d, 2H, J = 12.5 Hz, Xyl^1-*ortho*), 6.84 (s, 1H, Xyl^1-*para*), 7.26−7.35 (m, 5H, Cp-*Ph*), 7.38 (s, 1H, Xyl^2-*para*), 7.43−7.61 (m, 6H, P-Ph-*meta*, P-Ph-*para*), 7.74−7.89 (m, 4H, P-Ph-*ortho*), 8.18 (d, 2H, J = 12.5 Hz, Xyl^2-*ortho*). $^{13}C\{^1H\}$ NMR (100 MHz): δ 21.16 (2C, Xyl^1-CH_3), 21.50 (2C, Xyl^2-CH_3), 24.80−25.29 (m, CH_2), 66.06 (dd, J = 63.4 Hz, J = 9.3 Hz, Cp-C1), 69.75−69.93 (m, Cp-C4), 71.95 (br s, 5C, Cp′), 72.98 (d, J = 3.8 Hz, Cp-C5), 85.18 (d, J = 16.3 Hz, Cp-C3), 92.50 (t, J = 6.9 Hz, Cp-C2), 126.03 (d, J = 55.8 Hz, P-Ph-*ipso*), 127.55 (d, 2C, J = 3.8 Hz, P-Ph^1-*meta*), 127.65 (Cp-Ph-*para*), 128.22 (d, J = 54.1 Hz, P−Ph-*ipso*), 128.28 (2C, Cp-Ph-*meta*), 129.10 (d, 2C, J = 9.8 Hz, P−Ph^2-*meta*), 129.19 (d, 2C, J = 10.7 Hz, Xyl^1-*ortho*), 129.83 (2C, Cp-Ph-*ortho*), 130.29 (d, J = 51.8 Hz, P-Xyl-*ipso*), 131.33 (d, 2C, J = 3.0 Hz, P-Ph^1-*para* + P-Ph^2-*para*), 132.14 (d, J = 3.0 Hz, Xyl^1-*para*), 132.26 (d, J = 58.8 Hz, P-Xyl-*ipso*), 133.73 (d, 2C, J = 11.5 Hz, P-Ph^1-*ortho*), 134.25 (d, J = 3.0 Hz, Xyl^2-*para*), 134.54 (d, 2C, J = 11.5 Hz, P-Ph^2-*ortho*), 134.80 (d, 2C, J = 11.5 Hz, Xyl^2-*ortho*), 135.48 (Cp-Ph-*ipso*), 137.77 (d, J = 12.2 Hz, P-Xyl-Cq), 138.88 (d, J = 11.6 Hz, P-Xyl-Cq). P-Ph^1 and P-Ph^2, Cp-Ph-*meta* and Cp-Ph-*ortho*, as well as P-Ph-*ipso* and P-Xyl-*ipso*, interchangeable. $^{31}P\{^1H\}$ NMR (162 MHz): δ +23.14 (d, J = 7.9 Hz), +29.36 (d, J = 7.9 Hz).

[$PdCl_2$((*R*$_p$)-12c)]. Yield: 40%. Mp: dec >210 °C. $[\alpha]_\lambda^{20}$ (nm): +27 (589), +36 (578), +91 (546) (*c* 0.135, $CHCl_3$). ^1H NMR (400 MHz): δ 2.01 (s, 6H, Xyl^1-CH_3), 2.34 (s, 6H, Cp-Xyl-CH_3), 2.55 (s, 6H, Xyl^2-CH_3), 2.70 (dd, 1H, J = 16.1 Hz, J = 7.0 Hz, CH_2), 3.68 (s, 5H, Cp′), 3.72−3.84 (m, 1H, CH_2), 3.83 (t, 1H, J = 2.0 Hz, Cp-H5), 4.59−4.61 (m, 1H, Cp-H4), 6.50 (d, 2H, J = 12.4 Hz, Xyl^1-*ortho*), 6.85 (s, 1H, Xyl^1-*para*), 6.87 (s, 2H, Cp-Xyl-*ortho*), 6.94 (s, 1H, Cp-Xyl-*para*), 7.36 (s, 1H, Xyl^2-*para*), 7.43−7.59 (m, 6H, Ph-*meta*, Ph-*para*), 7.74−7.84 (m, 4H, Ph-*ortho*), 8.12 (d, 2H, J = 12.4 Hz, Xyl^2-*ortho*). $^{13}C\{^1H\}$ NMR (100 MHz): δ 21.19 (2C, Xyl^1-CH_3), 21.50 (2C, Cp-Xyl-CH_3), 21.67 (2C, Xyl^2-CH_3), 70.01−70.21 (m, Cp-C4), 71.84 (br s, 5C, Cp′), 72.84 (d, J = 3.8 Hz, Cp-C5), 84.59 (dd, J = 16.8 Hz, J = 2.3 Hz, Cp-Cq), 126.96 (d, J = 54.75 Hz, P-Ph-*ipso*), 127.62 (d, 2C, J = 10.7 Hz, P-Ph^1-*meta*), 127.67 (2C, Cp-Xyl-*ortho*), 129.12 (d, 2C, J = 10.7 Hz, P-Ph^2-*meta*), 129.14 (d, J = 67.3 Hz, P-Xyl-*ipso*), 129.27 (d, 2C, J = 11.5 Hz, Xyl^1-*ortho*), 129.32 (Cp-Xyl-*para*), 130.43 (d, J = 52.51 Hz, P-Ph-*ipso*), 131.29 (d, 2C, J = 3.0 Hz, P-Ph^1-*para* + P-Ph^2-*para*), 132.03 (d, J = 58.1 Hz, P-Xyl-*ipso*), 132.14 (d, J = 3.0 Hz, Xyl^1-*para*), 133.76 (d, 2C, J = 10.7 Hz, P-Ph^1-*ortho*), 134.36 (d, J = 3.0 Hz, Xyl^2-*para*), 134.40 (d, 2C, J = 11.5 Hz, P-Ph^2-*ortho*), 134.71 (d, 2C, J = 10.7 Hz, Xyl^2-*ortho*), 135.29 (Cp-Xyl-*ipso*), 137.73 (d, 2C, J = 12.0 Hz, P-Xyl-Cq), 137.83 (2C, Cp-Xyl-Cq), 138.66 (d, 2C, J = 12.0 Hz, P-Xyl-Cq). P-Ph^1 and P-Ph^2 as well as P-Ph-*ipso* and P-Xyl-*ipso* interchangeable. CH_2 and two Cp-Cq signals not observed. $^{31}P\{^1H\}$ NMR (162 MHz): δ +22.79 (d, J = 7.9 Hz), +30.34 (d, J = 7.9 Hz).

Standard Procedure for Hydrogenation Reactions. The substrate (2.53 mmol) and the catalyst (formed *in situ*, see below) were dissolved separately in the appropriate solvent (5 mL) under argon (total volume: 10 mL). The catalyst solution was stirred for 15 min. Both the catalyst and the substrate solution were transferred through a steel capillary into a 180 mL thermostated glass reactor or a 50 mL stainless steel autoclave. The inert gas was then replaced by hydrogen (three cycles), and the pressure was set. After completion of the reaction (total reaction times 1−20 h), the conversion was determined by gas chromatography and the product was recovered quantitatively after filtering the reaction solution through a plug of silica to remove the catalyst. The enantiomeric purity of the product was determined either by gas chromatography or by HPLC.

The following reaction conditions and methods for ee determination were applied:

MAC: 2.53 mmol (0.25 mol/L) of MAC; $[Rh(NBD)_2][BF_4]$ + 1.05 equiv of ligand; s/c = 200; solvent: MeOH (10 mL); $p(H_2)$: 1 bar; 25 °C; reaction time: 1 h. ee: GC; Chirasil-L-Val, 170 °C, isotherm.

DMI: 2.53 mmol (0.25 mol/L) of DMI; $[Rh(NBD)_2][BF_4]$ + 1.05 equiv of ligand; s/c = 200; solvent: MeOH (10 mL); $p(H_2)$: 1 bar; 25 °C; reaction time: 1 h. ee: GC; Lipodex E, 80 °C, isotherm.

MCA: 2.53 mmol (0.25 mol/L) of MCA; $[Rh(NBD)_2][BF_4]$ + 1.05 equiv of Ligand; s/c = 200; solvent: MeOH (10 mL); $p(H_2)$: 5 bar; 25 °C; reaction time: 16 h. ee: as methyl ester; HPLC; Chiralcel OB, Hex/*i*-PrOH: 98:2, 0.1 mL/min.

EAC: 2.53 mmol (0.25 mol/L) of EAC: $[Rh(NBD)_2][BF_4]$ + 1.05 equiv of ligand; s/c = 200; solvent: EtOH (9.5 mL); CF_3CH_2OH (0.5 mL); $p(H_2)$: 1 bar; 25 °C; reaction time: 16 h. ee: GC; Lipodex E, 130 °C, isotherm.

MPG: 2.53 mmol (0.25 mol/L) of MPG; $[Rh(NBD)Cl]_2$ + 2.1 equiv of ligand; s/c = 200; solvent: toluene (10 mL); $p(H_2)$: 80 bar; 25 °C; reaction time: 20.5 h. ee: HPLC; Chrialcel OJ, Hex/*i*-PrOH: 90:10, 1.0 mL/min.

EOP: 2.53 mmol (0.25 mol/L) of EOP; $[RuI_2(p\text{-cymene})]_2$ + 2.1 equiv of ligand (no pretreatment); s/c = 200; solvent: ethanol (10 mL); additive: 1 N HCl(aq), 60 μL; $p(H_2)$: 80 bar; 80 °C; reaction time: 16 h. ee: as TFA derivative; GC, Lipodex E, 80 °C, isotherm.

X-ray Structure Determination. Crystals of [$PdCl_2$(**9c**)], [$PdCl_2$(**10c**)], and [$PdCl_2$(**11c**)] in the form of [$PdCl_2$(**9c**)]·(1/2CH_2Cl_2,1/2C_2H_5OH), [$PdCl_2$(**10c**)]·solv, and [$PdCl_2$(**11c**)]·CH_2Cl_2 were obtained by slow diffusion of Et_2O into a solution of the corresponding complex in CH_2Cl_2 or CH_2Cl_2/C_2H_5OH ([$PdCl_2$(**9c**)]). In the case of [$PdCl_2$(**3**)] this procedure yielded only unsuitable thin needles. However, when this complex was crystallized from a highly concentrated solution in 1,2-dichlorethane, a small plate-like crystal of [$PdCl_2$(**3**)]·2$C_2H_4Cl_2$ was recovered from a polycrystalline mass. Crystal data and experimental details are given in Table 3. X-ray data were collected on Bruker Smart CCD area detector diffractometers using graphite-monochromated Mo Kα radiation (λ = 0.71073 Å) and 0.3° ω-scan frames covering complete spheres of the reciprocal space. Corrections for absorption, $\lambda/2$ effects, and crystal decay were applied.[23] The structures were solved by direct methods using the program SHELXS97.[24] Structure refinement on F^2 was carried out with the program SHELXL97.[24] All non-hydrogen atoms were refined anisotropically. Hydrogen atoms were inserted in idealized positions and were refined riding with the atoms to which they were bonded. Solvent disorder was taken into account. Thus, for [$PdCl_2$(**3**)]·2CH_2Cl_2 and [$PdCl_2$(**10c**)]·solv (solv = mainly

(23) Bruker programs: *SMART*, version 5.629; *SAINT*, version 6.45; *SADABS*, version 2.10; *XPREP*, version 6.1; *SHELXTL*, version 6.14; Bruker AXS Inc.: Madison, WI, 2003.

(24) Sheldrick, G. M. *SHELX97*: Program System for Crystal Structure Determination; University of Göttingen: Göttingen, Germany, 1997.

Et_2O) the solvents were squeezed with the program PLATON.[25] For $[PdCl_2(\mathbf{3})]\cdot 2C_2H_4Cl_2$ the cyclopentadienyl and benzene rings were idealized.

Acknowledgment. This work was kindly supported by Solvias AG, Basel.

Supporting Information Available: Details on the synthesis of all ligands as well as complete crystallographic data and technical details in CIF format for compounds $[PdCl_2(\mathbf{3})]\cdot 2C_2H_4Cl_2$, $[PdCl_2(\mathbf{9c})]\cdot(CH_2Cl_2, C_2H_5OH)$, $[PdCl_2(\mathbf{10c})]\cdot$solv, and $[PdCl_2(\mathbf{11c})]\cdot CH_2Cl_2$. This material is available free of charge via the Internet at http://pubs.acs.org.

OM700405A

(25) Spek, A. L. *PLATON*: A Multipurpose Crystallographic Tool; University of Utrecht: Utrecht, The Netherlands, 2005.